Comprehensive map and functional annotation of the Mouse White Adipose Tissue Proteome

Xiao-yue Tang [Equal first author, 1], Juan Li [Equal first author, 2], Wei-gang Zhao [2], Hai-dan Sun [3], Zheng-guang Guo [3], Jing Li [3], Zhu-fang Shen [4], Tao Yuan [2], Shuai-nan Liu [4], Quan Liu [4], Yong Fu [2], Wei Sun [Corresp. 1]

[1] Core Facility of Instrument, Institute of Basic Medical Sciences, Chinese Academy of Medical Sciences/School of Basic Medicine, Beijing, China

[2] Department of Endocrinology, Key Laboratory of Endocrinology of Ministry of Health, Peking Union Medical College Hospital, Chinese Academy of Medical Science and Peking Union Medical College, Beijing, China

[3] Core Facility of Instrument, Institute of Basic Medical Sciences, Chinese Academy of Medical Sciences/School of Basic Medicine, Peking Union Medical College, Beijing, China

[4] State Key Laboratory of Bioactive Substances and Functions of Natural Medicines, Institute of Materia Medica, Chinese Academy of Medical Sciences and Peking Union Medical College, Diabetes Research Center of Chinese Academy of Medical Sciences, Beijing, China

Corresponding Author: Wei Sun
Email address: sunwei@ibms.pumc.edu.cn

White adipose tissue (WAT) plays a significant role in energy metabolism and the obesity epidemic. In this study, we sought to (1) profile the mouse WAT proteome with advanced 2DLC/MS/MS approach, (2) provide insight into WAT function based on protein functional annotation and (3) predict potential secreted proteins. A label-free 2DLC/MS/MS proteomic approach was used to identify the WAT proteome from female mouse WAT. A total of 6039 proteins in WAT were identified, among which 5160 were quantified (spanning a magnitude of 10^6) using an intensity-based absolute quantification algorithm , and 3117 proteins were reported by proteomics technology for the first time in WAT. To comprehensively analyze the function of WAT, the proteins were divided into three quantiles based on abundance and we found that proteins of different abundance performed different functions . High-abundance proteins (the top 90%, 1219 proteins) were involved in energy metabolism; middle-abundance proteins (90%-99%, 2273 proteins) were involved in the regulation of protein synthesis; and low-abundance proteins (99%-100%, 1668 proteins) were associated with lipid metabolism and WAT beiging. Furthermore, 800 proteins were predicted by SignalP4.0 to have signal peptides, 265 proteins had never been reported, and 5 have been reported as adipokines. The above results provide a large dataset of the normal mouse WAT proteome , which might be useful for WAT function research.

Comprehensive Map and Functional Annotation of the Mouse White Adipose Tissue Proteome

Xiao-Yue Tang[1#], Juan Li[2#], Wei-Gang Zhao[2*], Hai-Dan Sun[1], Zheng-Guang Guo[1], Jing Li[1], Zhu-Fang Shen[3], Tao Yuan[2], Shuai-Nan Liu[3], Quan Liu[3], Yong Fu[2], Wei Sun[1*]

[1] *Core Facility of Instrument, Institute of Basic Medical Sciences, Chinese Academy of Medical Sciences/School of Basic Medicine, Peking Union Medical College, Beijing, China*

[2] *Department of Endocrinology, Key Laboratory of Endocrinology of Ministry of Health, Peking Union Medical College Hospital, Chinese Academy of Medical Science and Peking Union Medical College, Beijing, China*

[3] *State Key Laboratory of Bioactive Substances and Functions of Natural Medicines, Institute of Materia Medica, Chinese Academy of* Medical *Sciences and Peking Union Medical College, Diabetes Research Center of Chinese Academy of Medical Sciences, Beijing, China*

\# Contributed equally to this work

* Corresponding authors

[*] xiehezhaoweigang@163.com (WGZ); sunwei@ibms.pumc.edu.cn (WS)

Abstract

White adipose tissue (WAT) plays a significant role in energy metabolism and the obesity epidemic. In this study, we sought to (1) profile the mouse WAT proteome with advanced 2DLC/MS/MS approach, (2) provide insight into WAT function based on protein functional annotation and (3) predict potential secreted proteins. A label-free 2DLC/MS/MS proteomic approach was used to identify the WAT proteome from female mouse WAT. A total of 6039 proteins in WAT were identified, among which 5160 were quantified (spanning a magnitude of 10^6) using an intensity-based absolute quantification algorithm, and 3117 proteins were reported by proteomics technology for the first time in WAT. To comprehensively analyze the function of WAT, the proteins were divided into three quantiles based on abundance and we found that proteins of different abundance performed different functions. High-abundance proteins (the top 90%, 1219 proteins) were involved in energy metabolism; middle-abundance proteins (90%-99%, 2273 proteins) were involved in the regulation of protein synthesis; and low-abundance proteins (99%-100%, 1668 proteins) were associated with lipid metabolism and WAT beiging. Furthermore, 800 proteins were predicted by SignalP4.0 to have signal peptides, 265 proteins had never been reported, and 5 have been reported as adipokines. The above results provide a large dataset of the normal mouse WAT proteome, which might be useful for WAT function research.

KEYWORDS: White adipose tissue; Proteome; Mouse; Label-free

Introduction

35

36 Mammals have two types of adipose tissue, brown adipose tissue (BAT) and white adipose

37 tissue (WAT). BAT dissipates energy and increases fatty acid oxidation and heat production by

38 uncoupled respiration, which is mediated by uncoupling protein-1 (UCP1) [1, 2]. The primary

39 function of WAT is to store energy in lipid droplets in the form of triacylglycerols (TAGs) [3].

40 WAT also secrete hormones and cytokines to regulate energy intake, energy expenditure, and

41 carbohydrate and lipid metabolism, e.g., adiponectin, leptin, and plasminogen activator inhibitor-

42 1 [4]. Furthermore, many studies have found that these hormones and cytokines are associated

43 with diseases. For example, adiponectin (ADI), one of the most abundant adipokines produced by

44 adipocytes, plays a fundamental role in maintaining vascular homeostasis, protecting from

45 vascular injury and atherogenesis [5, 6]. These proteins are considered a valuable resource in

46 disease research. Therefore, a comprehensive profile of the WAT proteome will provide a basic

47 understanding of WAT function and benefit disease studies.

48 The earliest study of the normal WAT proteome was from Sanchez et al. in 2001 [7]. In this

49 study, 61 protein entries from mouse WAT were identified from one hundred and nine spots in a

50 2D-PAGE gel. Later, to optimize the resolution of WAT proteins, Lanne et al. used thiourea to

51 obtain distinct spots in a 2D gel and finally identified 108 proteins from 140 spots in a 2D gel

52 taken from the WAT of the epididymal fat pads of obese, diabetic ob/ob mice [8]. In 2013, Cheng-

53 Hsien et al. analyzed proteins differentially expressed in the WAT of mice fed diets with or without

54 bitter melon seed oi for 11 weeks using two dimensional gel electrophoresis and finally identified

55 23 proteins from 30 spots[9].With the development of mass spectrometry technology, more

56 proteins can be identified in WAT. In 2007, Adachi et al. [10] investigated the adipocyte proteome

57 by combining one-dimensional gel electrophoresis and on-line electrospray tandem mass

58 spectrometry with biochemical procedures for the subfractionation of the 3T3-L1 adipocyte

59 cellular proteome (nuclei, mitochondria, membrane, and cytosol). Finally, they reported 3287

60 SwissProt annotated proteins in 3T3-L1 adipocytes. In 2009, Forner et al. [11] analyzed the mouse

61 fat mitochondria proteome response to cold-induced thermogenesis. By combining HPLC and

62   high-resolution quantitative linear ion trap (LTQ)-Orbitrap mass spectrometry with the SILAC

63   method, they identified 2434 proteins from the mitochondria of mouse adipose tissue. In 2010, Xie

64   et al. [12] identified 1493 adipocyte proteins isolated from abdominal adipose tissue using a one-

65   dimensional SDS-PAGE and HPLC-ESI-MS/MS approach. In 2018, Peter et al. [13] analyzed

66   mesenteric, omental, and uterine adipose tissue groups from the peritoneal cavities of young and

67   aged C57BL/6J mouse cohorts with SDSPAGE gel combination with LC-MS/MS method. They

68   finally identified 2308 protein groups and quantified 2167 groups. There were also some studies

69   to investigate differently expressed proteins in adipose tissue to unveil the mechanisms underlying

70   adipose tissue dysfunction and understand the functional mechanism of WAT[14-17].

71   Presently, due to its high-throughput and high-sensitivity capacities, proteomics technology

72   has garnered a lot of attention recently in biological research. The number of identified gene

73   products in two proteome studies of human tissues and body fluids even approached the number

74   of protein-coding genes in the complete human genome [18-20].

75   Therefore, in this study, we sought to (1) profile the mouse WAT proteome with advanced

76   2DLC/MS/MS approach, (2) provide insight into WAT function based on protein functional

77   annotation and (3) predict potential secreted proteins. In previous reports of WAT proteome, SDS-

78   PAGE was the most commonly used method for protein separation, but its peak capacity was limit.

79   2DLC approach could greatly improve the peak capacity by the orthogonality of the two-

80   dimensional separations, therefore, it could identify more proteins [21-23]. Thus, 2DLC approach

81   was used in our study. For mass spectrometer, Triple TOF 5600 with higher sensitivity and

82   resolution was used in the present study. To this end, we performed an in-depth WAT proteomic

83   analysis using normal mouse WAT samples. Qualitative and quantitative analysis were applied to

84   comprehensively profile the mouse WAT proteome. The function of WAT and the potentially

85   secreted protein prediction was annotated with bioinformatic analysis. Our data provides a

86   comprehensive mouse WAT proteome dataset, which might be useful for WAT function research.

Experimental procedures

1. Animals

Six- to eight-week-old female C57BL/6J mice were purchased from HFK Bioscience Laboratories (Beijing, China). All mice were maintained with free access to water and food and maintained under SPF conditions and a 12 h light/dark cycle at $23 \pm 2°C$. The mice were fed with a standard chow (SC; 10% lipids) diet for 22 weeks. All animals were handled according to the Standards for Laboratory Animals (GB14925-2001) and the Guideline on the Humane Treatment of Laboratory Animals (MOST 2006a) established by the People's Republic of China. The two guidelines were conducted in adherence to the regulations of Institutional Animal Care and Use Committee (IACUC) and all animal procedures were approved by IACUC (approval number: SCXKBeijing- 2009-0004). All efforts were made to minimize suffering.

2. Preparation of WAT samples

A total of 6 C57BL/6J mice was applied to collect 300 mg gonadal WAT. Phosphate buffer solution (PBS) was used to wash the tissue. The tissues were gently agitated by vortexing, and centrifuged at 1000 g for five minutes. After the solution was removed. 1 mL lysis buffer (protein extraction kit, P1250-50, Applygen, Beijing) and 1 μL protease inhibitor cocktail (50x, P1265-0.5, Applygen, Beijing) (1:1000) were added to the tissue. And the tissue was homogenized using a spinning blade tissue homogenizer (IKA R104, Janke & Kunkel KG.IKA-werk, Germany) on ice for complete lysis. 2mL protein extraction regent were added to the tissue and kept in 4 ℃ for 40 minutes to separate lipid completely. After centrifugation at 4℃ for 10 minutes, the solution is divided into two phases and the middle of the two phases is protein membrane. The upper and lower two layers of liquid are removed and the protein membrane is attached to the centrifugal tube wall. Protein dissolution was performed by adding a buffer solution containing 7 M urea, 2 M thiourea, 65 mM DTE, and 83 mM Tris (Sigma-Aldrich, St. Louis, MO, USA). After 10 min of $20,000 \times g$ centrifugation at 4°C, the supernatants were collected and stored at -80°C. The Bradford assay with Bradford reagents (Thermo Fischer Scientific, USA) was supplied to measure the protein concentration of the WAT samples. The six WAT protein samples were pooled into one

115 mixed sample with the same protein amount. The WAT proteins were prepared using filter-aided

116 sample preparation methods [24]. The sample (100 μg in total) was deoxidized with 20 mM DTT

117 and alkylated with 50 mM IAA. Then, the WAT proteins were loaded onto a 10 kDa filter device

118 (micro Biospin, Nanosep 10K Omega; PALL, USA) and centrifuged at 14,000 g at 4°C. After

119 washing twice with UA (8 mol/L urea in 0.1 mol/L Tris-HCl, pH 8.5) and four times with 25

120 mmol/L NH_4HCO_3, the samples were digested with trypsin (Trypsin Gold, mass spec grade,

121 Promega, WI, USA, enzyme to protein ratio of 1:50) and incubated at 37 °C overnight. After

122 digestion, HLB 3 cc extraction cartridges (Oasis, Waters, Ireland) were applied to desalt the

123 peptides. 500 μl 0.1% formic acid cleaned the peptide three times and peptide was finally eluded

124 with 500 μL 100% ACN. The pooled peptide elution was vacuum dried and stored at -80°C.

125 **3. LC-MS/MS**

126   The pooled peptide mixture was first fractioned using a high-pH RPLC column from Waters

127 (4.6 mm×250 mm, C_{18}, 3 μm). The sample was loaded onto the column in buffer A1 (pH = 10).

128 Peptides were separated and eluted from 5% B1 to 90% B1 (90% ACN; pH = 10, flow rate, 1

129 mL/min) in 60 min. The eluted peptides were collected at a rate of one fraction per minute and we

130 concatenated the 60 collected fractions into 20 fractions (concatenation scheme: 1 + 21 + 41, 2 +

131 22 + 42, etc.). Each pooled sample was analyzed on a RP-C_{18} self-packing LC column (75 μm×100

132 mm, 3 μm). The eluted gradient was 5–30% buffer B2 (0.1% formic acid, 99.9% ACN; flow rate,

133 0.5 μL/min) for 60 min.

134   The eluted peptide was measured using LC-MS instrumentation consisting of a nano source to

135 TripleTOF 5600 mass spectrometer. High sensitivity mode and the following parameters were

136 used when acquiring the MS/MS data. MS data were acquired with 30 data-dependent MS/MS

137 scans per every full scan and full scans were acquired at a resolution of 40,000 and MS/MS scans

138 at 20,000. 35% normalized collision energy and charge state screening (including precursors with

139 +2 to +4 charge state) was applied. MS/MS scans were performed at the scan range of m/z 100–

140 1800 with the scan time of 100 ms. Dynamic exclusion was set to 15 s to avoid repeated sequencing

141 of identical peptides.

142 **4. Data processing**

143   The MS/MS spectra were processed using Mascot software (version 2.3.02, Matrix Science,

144 London, UK) and searched against the SwissProt mouse database from the UniProt website

145 (http://www.UniProt.org). The specificity of trypsin digestion was set for cleavage after K or R

146 and two missed cleavage sites in the trypsin digestion were allowed. The fixed modification was

147 carbamidomethylation of cysteine in Mascot. Deamidation of asparagine and glutamine and the

148 oxidation of methionine were specified as variable modifications. The parent ion tolerance was set

149 to 10 ppm and the fragment ion mass tolerance was set to 0.05 Da. Mascot search results were

150 further validated using Scaffold (version 4.3.2, Proteome Software Inc., Portland, OR). Peptide

151 identifications were accepted at an FDR less than 1.0% by the Scaffold Local FDR algorithm and

152 were determined by searching a reverse database. Proteins that contained similar peptides and

153 could not be differentiated based on MS/MS analysis alone were grouped to satisfy the principles

154 of parsimony. Proteins sharing significant peptide evidence were grouped into clusters. Protein

155 identifications were accepted if they could achieve a false discovery rate (FDR) of less than 1.0%

156 and contain at least 2 uniquely identified peptides.

157   To rank the relative abundance of proteins, an intensity-based absolute quantification (iBAQ)

158 algorithm was used [25]. The detailed protocol was provided below:

159   (1) The protein intensities were first computed by Progenesis LC–MS (v2.6, Nonlinear

160 Dynamics, UK) as the sum of all identified peptide intensities (maximum peak intensities of the

161 peptide elution profile, including all peaks in the isotope cluster).

162   (2) The protein intensities were then divided by the number of theoretically observable peptides

163 (calculated by in silico protein digestion; all fully tryptic peptides between 6 and 30 amino acids

164 were counted). The resulting intensities were iBAQ values. which are shown as "Absolute iBAQ

165 intensities".

166   (3) The relative iBAQ intensities were computed by dividing the absolute iBAQ intensities by

167 the sum of all absolute iBAQ intensities.

168   (4) The relative iBAQ intensities were applied to estimate the estimated protein abundances

169   (the proportions of protein amounts to total WAT protein amount). The estimated protein

170   abundances in WAT were finally calculated by multiplying the relative iBAQ intensities by

171   theoretically relative molecular mass.

172   (5) The percentage was computed by dividing the estimated protein abundances by the sum of

173   all estimated protein abundances.

174   **5. Functional annotation**

175   Gene Ontology (GO) was performed using the PANTHER database (Protein Analysis through

176   Evolutionary Relationships, http://www.pantherdb.org/). Proteins were divided into cellular

177   components, biological processes, and molecular functions based on their functional annotations.

178   When more than one assignment was available, all the functional annotations were considered in

179   the results.

180   The Ingenuity Pathway Analysis (IPA, Ingenuity Systems, Mountain View, CA) database was

181   used to analyze canonical pathways. The SwissProt accession numbers of the identified proteins

182   were uploaded into the IPA using default settings. This analysis was focused on the pathways and

183   functions in which the proteins are expected to be involved. All identified WAT proteins, high,

184   middle and low-abundance proteins were analyzed respectively.

185   All proteins were used for potential secreted protein prediction. For this purpose, the SwissProt

186   accession numbers were input into SignalP 4.1 (http://www.cbs.dtu.dk/services/SignalP/) [17].

187   This software was used to predict the N-terminal signal peptides for classically secreted proteins.

188

189   **Results**

190   **1. Workflow of proteome analysis**

191   In this study, samples of WAT from six C57BL/6J female mice were used to generate a

192   comprehensive profile of the normal mouse WAT proteome. The extracted proteins were digested

193   using the filter-aided sample preparation (FASP) method [24]. The digested peptides were first

194   separated by high-pH RPLC and mixed into 20 fractions and analyzed by nanoRPLC−MS/MS in

195   three replicates. The peak intensity-based semiquantification method iBAQ was used to estimate

196   the abundance of the quantified proteins. The PANTHER classification system and IPA were

197   applied to annotate the function of WAT. The SignalP 4.1 Server was applied to predict secreted

198   proteins **(Supplemental Fig.S1)**.

199   **2. A comprehensive profile of the WAT proteome**

200   In this study, pooled WAT samples were used to establish a large database for the WAT

201   proteome. All of 516,703 spectra, 60,215 unique peptides and 6,039 proteins were identified

202   (FDR<1% at the protein and peptide level with at least two unique peptides for each protein)

203   **(**Detailed data provided in **Tables S1 - S3)**. Among the 6039 identified proteins, 77% had

204   molecular weight between 10kD-90kD **(Supplemental Fig.S2)**. 5057 proteins (84%) of the 6039

205   proteins were identified in the three replicates **(Fig. 1A)**.

206   In order to improve our understanding of the WAT proteome and facilitate the development of

207   WAT functional annotation, quantitation of WAT proteins was performed. Among the 6039

208   identified proteins, 5270 proteins could be quantified by the peak intensity-based semi-

209   quantification method iBAQ [25] **(Fig. 1B)**. As for the correlation of protein quantification, the

210   correlation of two replicates was approximately 0.98 **(Supplemental Fig.S3),** indicating good

211   LC/MS/MS reproducibility. The proteins with technical CVs greater than 0.3 were excluded from

212   further analysis in order to reduce the interference of technical variation, and a total of 5160 WAT

213   proteins **(Fig. 1C, Table S4)** were kept. The relative protein abundance spans 6 orders of

214   magnitude**.** We divided the quantified proteins into three quantiles based on protein abundance:

215   high- (the top 90%, 1219 proteins), middle- (90%-99%, 2273 proteins) and low-abundance

216   proteins (99%-100%, 1668 proteins). Additionally, Table 1 listed top ten abundant proteins

217   quantified with the iBAQ algorithm in our research. The ten proteins account for 20% of the total

218   WAT protein abundance. Carbonic anhydrase 3, vimentin and polymerase I and transcript release

219   factors are associated with fatty acid metabolism, adipogenesis and lipolysis, respectively [26-28].

220   Galectin-1 (GAL1) has been proposed as an early marker of adipocyte differentiation and to be

221   actively involved in adipose tissue development [29, 30]. The expression of transgelin was

222   associated with the development of white adipocyte, and thought to begin with progenitor cells

223   from the perivascular compartment (pericytes) in WAT [31]. Other three proteins, tropomyosin

224   (beta chain), desmin and myosin light polypeptide 6, were cytoskeletal proteins.

225   When comparing with previous studies **(Table 2, Fig.2A)**, approximately 58% of the fat

226   mitochondria proteome, 60% of the mesenteric, omental, and uterine adipose tissue proteome, 63%

227   of the 3T3-L1 adipocyte proteome and 92% of the adipocyte proteome (isolated from abdominal

228   adipose tissue) was overlapped with our study, respectively. When all data from these four studies

229   were combined, 352 proteins were detected in all of the studies and 3117 proteins from our results

230   were reported for the first time by proteomics technology in WAT. Among common proteins

231   (**Fig.2B**), high- and middle-abundance proteins contributed about 84%. And among specific

232   proteins, less (7%) high-abundance proteins were found in our study. When comparing previous

233   study with our high-abundance proteins (**Supplemental Fig.S4**), 177 proteins were firstly reported

234   in our study and 85% (1042 proteins) of our high-abundance proteins could be identified

235   previously. The above data showed that most high abundance proteins (85%) and middle

236   abundance proteins (52%) were identified by previous reports, and less proteins low abundant

237   proteins (26%). The possible reasons might come from the proteome approach. Due to the

238   limitations of separation method and mass spectrometer in previous studies, most identified

239   proteins in previous reports were high or medium ones, therefore, these proteins had more chances

240   to be identified in our study.

241   **3. The functional annotation of the WAT proteome**

242   To explore the function of WAT more comprehensively, PANTHER classification system

243   (http://www.pantherdb.org/genes/batchIdSearch.jsp) and IPA tool (http://www.ingenuity.com/)

244   were applied to the functional classification and pathway analysis.

245   The identified proteins were functionally categorized using Gene Ontology annotation terms.

246   As shown in **Fig. 3A**, nearly 85% of the proteins were present in cells, including cell part (40.6%,

247   including intracellular part and endomembrane system), organelles (26.3%, including intracellular

248   organelle and non-membrane bounded organelle) and macromolecular complex (17.4%, including

249   membrane protein complex, catalytic complex and ribonucleoprotein complex). The major

250   molecular functions of WAT proteins were catalytic activity (44%, including hydrolase activity

251   and transferase activity) and binding (37.5%, including protein binding and heterocyclic

252   compound biding). High-abundance proteins were enriched with antioxidant activity (5.9%) and

253   structural molecular activity (10.1%) when compared with the middle and low-abundance proteins

254   **(Fig. 3B)**. Using iBAQ analysis, the high-abundance proteins with antioxidant and catalytic

255   activity accounted for 35% of all the high-abundance proteins, and the abundance of proteins with

256   structural molecular activity accounted for 8%. For biological processes **(Fig. 3C)**, approximately

257   half of the WAT proteins were associated with metabolic processes (25.1%) and cellular processes

258   (31%). High-abundance proteins were enriched with cellular component organization or

259   biogenesis (11.3%), multicellular organismal process (4.5%) and biological adhesion functions

260   (1.7%). The above results show that energy metabolism is an important function of WAT.

261   To identify the major biological pathways involved with the identified proteins, IPA was used

262   for canonical pathway enrichment analysis **(Fig. 3D, Supplemental Fig. S5 and Table S5)**. The

263   functions of WAT include protein synthesis (such as the protein ubiquitination pathway, EIF2

264   signaling, mTOR signaling, and the regulation of eIF4 and p70S6K signaling), energy metabolism

265   (such as mitochondrial dysfunction, sirtuin signaling, PI3K/AKT signaling, and oxidative

266   phosphorylation), adipogenesis (such as PI3K/AKT signaling) and the regulation of insulin action

267   (such as integrin signaling). The function of the high-abundance proteins was mainly related to

268   energy metabolism (mitochondrial dysfunction, oxidative phosphorylation, and sirtuin signaling).

269   The primary function of the middle-abundance proteins was protein synthesis (mTOR signaling,

270   regulation of eIF4 and p70S6K signaling, EIF2 signaling and tRNA charging). The functions of

271   low-abundance proteins were WAT beiging (NGF and IL-4 signaling) and lipid metabolism (super

272   pathway of inositol phosphate compounds, 3-phosphoinositide degradation and 3-

273   phosphoinositide biosynthesis).

274   **4. The analysis of WAT secreted proteins**

275   Endocrine function is one of the key roles of adipocytes, and adipose tissue can synthesis

276   several hormones, called adipokines or adipocytokines. We applied the SignalP 4.1 Server to

277   predict potential secreted proteins. In all, 800 proteins were found to have signal peptides **(Table**

278   **S6),** of which 200 proteins belong to the high-abundance proteins, 312 belong to the middle-

279   abundance proteins and 183 belong to the low-abundance proteins. The abundance of all the

280   proteins with signal peptides was 15.6% in the WAT proteome. In 2018, Ali et al. identified 453

281   proteins from adipocytes that had previously been reported to be secreted proteins [32], of which

282   265 proteins were found in our results. Moreover, 5 WAT proteins were confirmed as adipokines:

283   resistan, adiponectin, apolipoprotein E, haptoglobin and angiotensinogen [33-35].

284   In addition, the peak intensity-based semiquantification method iBAQ was applied to estimate

285   the abundance of the identified 800 proteins, of which 694 proteins could be quantified [36]. The

286   relative protein amounts span 5 orders of magnitude, from Semaphorin-4A (9.74E-01) to alpha-2-

287   HS-glycoprotein (3.81E+04) (**Fig. 2C**).

288

Discussion

289

290   White adipose tissue(WAT) stores energy in lipid droplets in the form of TAGs[3] and secrete

291   hormones and adipokines to regulate energy intake, energy expenditure, and carbohydrate and

292   lipid metabolism [4]. A comprehensive profile of the WAT proteome will provide a basic

293   understanding of WAT function and benefit disease studies. In the present study, we established a

294   large database for the WAT proteome by advanced 2D LC-MS/MS. Total 6,039 proteins were

295   identified, of which 5270 proteins could be quantified by the peak intensity-based semi-

296   quantification method iBAQ. Functional annotation was further explored and we found that

297   proteins of different abundance performed different functions.

298   Canonical pathway enrichment analysis revealed that one of the primary functions of WAT

299   was protein synthesis, and related significant pathways was EIF2 signaling. Global translation and

300   apoptosis can be started by phosphorylation of EIF2-a [37] and eIF4E was released by

301   phosphorylation of eIF4E-BP binds to 5′ capped mRNAs to enhance their translation [38]. Another

302   significant WAT pathway is the PI3K/AKT signaling pathway, which plays a significant role in

303   phytol-enhanced adipogenesis and glucose uptake of adipocytes and lipolysis inhibition [39, 40].

304   These results show the synthetic metabolism function of WAT, which is consistent with the

305   traditional energy storage role of WAT [33]. Furthermore, a previous study has suggested that

306   adipose tissue plays an important role in insulin resistance [41]. In our result, integrin signaling

307   performed this function. A total of 103 proteins were found to be involved in this pathway, such

308   as Akt and ILK. ILK can interact with the integrin cytoplasmic domains, and integrins rely on ILK

309   for signal transduction. The pseudokinase domain of ILK is an important domain for the

310   recruitment of adaptor proteins and/or signaling molecules, such as Akt and PDK1. Integrins are

311   important regulators of insulin action and represent novel therapeutic targets to treat the underlying

312   insulin resistance associated with T2D [40].

313   The WAT proteome was divided into high, middle and low abundance proteins by iBAQ

314   quantitative method. According to IPA functional annotation high-abundance proteins was mainly

315   related to energy metabolism (mitochondrial dysfunction, oxidative phosphorylation, and sirtuin

316   signaling). Sixty-five proteins were involved in sirtuin signaling, such as sirt2. During energy

317   deficiency (caloric restriction or fasting) the expression of sirt2 increases [42, 43]. In this situation,

318   adipogenesis was suppressed and adipocyte lipolysis was increased to promote fuel availability by

319   sirt2 [42]. In another significant pathway, oxidative phosphorylation occurs in mitochondria and

320   comprises an electron-transfer chain, which is driven by substrate oxidation and is coupled to the

321   synthesis of ATP through an electrochemical transmembrane gradient. When energy needs

322   increase, fatty acid oxidation supplies an important source of energy for ATP production [44]. In

323   oxidative phosphorylation, 60% ubiquinone oxidoreductase (including NDUFS4, NDUFA3,

324   NDUFA4), 46% ubiquinol cytochrome c oxidoreductase (including UQCRFS, UQCRC2) and

325   63% ATP synthase (including ATP5A1, ATP5D) were high-abundance proteins (**Supplemental**

326   **Fig.S6A**). The other function of mitochondria is adipogenesis, which is accompanied by

327   mitochondrial biogenesis [45]. The mitochondria provides key intermediates for the synthesis of

328   triacylglycerolmight and further plays a critical role in lipogenesis [46]. For mitochondrial

329   dysfunction, many significant proteins were high-abundance proteins, including aconitase2 and

330   cytochrome c oxidase. Aconitase2 was an enzyme to catalyze the interconversion of citrate via cis-

331   aconitase in the second step of the TCA cycle. Cytochrome c oxidase was the terminal enzyme of

332   the mitochondrial respiratory chain and a multi-submit enzyme complex to transfer electrons in

333   mitochondrial (**Supplemental Fig.S6B**). These results showed that besides basic physiological

334   functions (structural molecular functions), high-abundance proteins also have important energy

335   metabolism functions in WAT.

336   IPA analysis showed that the primary function of the middle-abundance proteins was protein

337   synthesis (mTOR signaling, regulation of eIF4 and p70S6K signaling, EIF2 signaling and tRNA

338   charging). According to a previous study, protein synthesis is associated with adipogenesis [47].

339   The concentration of numerous mitochondrial proteins such as cytochrome c had a 20- to 30-fold

340   increase during differentiation of 3T3-L1 cells (a preadipocyte cell line). The expression of many

341   nucleus-encoded mitochondrial genes during adipogenesis was also found to have statistically

342   significant increases by mRNA profiles. The increase in mitochondrial proteins is not completely

343 achieved by enhanced transcription but is also involved in posttranscriptional regulation. Adipose

344 conversion (preadipocytes to adipocytes) would be accompanied by mitochondrial proliferation,

345 which underscores the essential role of mitochondria in the key aspects of lipid metabolism [47].

346 The functions of low-abundance proteins were WAT beiging (NGF and IL-4 signaling) and

347 lipid metabolism (super pathway of inositol phosphate compounds, 3-phosphoinositide

348 degradation and 3-phosphoinositide biosynthesis). NGF signaling plays a key role in the beiging

349 of WAT by regulating the plasticity of intra-adipose sympathetic arborizations in mouse inguinal

350 WAT in response to a cold challenge. Intra-adipose sympathetic plasticity was suppressed by the

351 blockage of NGF signaling, and moreover, the cold-induced beiging process of WAT was

352 suppressed[48]. IL-4 signaling is involved in the cold-induced biogenesis of beige fat. All of 22

353 proteins were found to be involved in this pathway, including STAT6. STAT6 is thought to be

354 necessary for the cold-induced remodeling of WAT into beige fat. Qiu et al. [49] found that cold-

355 induced expression of the protein UCP1 in subcutaneous WAT decreased by ~12-fold in Stat6-/-

356 mice, accompanied by an increase in oxygen consumption. Accordingly, Stat6-/- mice maintained

357 thermal homeostasis at a lower body temperature. Because beiging of WAT results in enhanced

358 energy expenditure, it has increasingly gained attention for its potential application in the

359 prevention and treatment of obesity and type 2 diabetes[50, 51].

360 In addition, 800 proteins were found to be secreted proteins in our result, of which 694 proteins

361 could be quantified by iBAQ. The top 5 newly identified (most abundant) secreted proteins were

362 carboxylesterase 1D, serine protease inhibitor A3K, apolipoprotein A-I, carboxylesterase 1C and

363 fibrillin-1.Carboxylesterase 1D, a major lipase in WAT, may mediate some or all hormone-

364 sensitive lipase -independent lipolysis in adipocytes[52]. Apolipoprotein A-I was associated with

365 cholesterol transport in high-density lipoprotein [53]. Fibrillin-1 was related with tissue

366 homeostasis [54]. It was reported to be up-regulated in the WAT of diet-induced obese mice [55],

367 which was affected by the structural changes when adipose tissue enlargement. The other two

368 proteins were serine protease inhibitor A3K and carboxylesterase 1C. Serine protease inhibitor

369 A3K was a contrapsin to inhibit trypsin-like proteases[56, 57]. Carboxylesterase 1C was involved

370 in the detoxification of xenobiotics and in the activation of ester and amide prodrugs and in the

371 extracellular metabolism of lung surfactant. No studies were reported to explore the correlation

372 between them and white adipose tissue. Their functions in WAT need more work.

373

374 **Conclusion**

375   In conclusion, using high-pH reverse-phase liquid chromatography (hp-RPLC) integrated with

376   a TripleTOF 5600 mass spectrometer, we provided the largest dataset from the normal mouse

377   WAT proteome up to now. Our WAT proteome included many proteins that had not been

378   previously reported by proteomic approach. We further provided insight into WAT function based

379   on protein functional annotation and found that proteins of different abundance performed

380   different functions. Finally, potential secreted proteins prediction was performed. Our data set

381   provided a comprehensive mouse WAT proteome, which might be useful for WAT function

382   research.

383   In the future, the following issues should be addressed: With the emergence of new instruments

384   (e.g., Orbitrap Fusion Lumos Tribrid mass spectrometer), labeling reagents (e.g., Ten-plex TMT

385   labeling) and new techniques (e.g., the Data Independent Acquisition technique), high-throughput

386   proteome analysis has come to fruition and might provide a more precise quantification and

387   functional analysis. Besides, multiple sample preparation methods and adipose tissue samples from

388   multiple regions will be needed to truly obtain a comprehensive WAT proteome. Furthermore,

389   with the development of genomics, transcriptomes, proteomics and metabolomics, the

390   combination of multiple omic analysis would lead to a better platform for routine clinical research.

391

392 **Acknowledgments**

393 This work was supported by   National Key Research and Development Program of China (No.

394 2016 YFC 1306300,2018YFC0910202,), National Natural Science Foundation of China (No.

395 30970650, 31200614, 31400669, 81371515, 81170665, 81560121), Beijing Natural Science

396 Foundation (No. 7173264, 7172076), Beijing cooperative construction project (No.110651103),

397 Beijing Science Program for the Top Young (No.2015000021223TD04), Beijing Normal

398 University (No.11100704), Peking Union Medical College Hospital (No.2016-2.27), CAMS

399 Innovation Fund for Medical Sciences (2017-I2M-1-009) and Biologic Medicine Information

400 Center of China, National Scientific Data Sharing Platform for Population and Health.

401 **Conflict of interest**

402 The authors declare no conflicts of interest.

403

References

404

405   1.   Klingenberg, M., *Uncoupling protein--a useful energy dissipator.* J Bioenerg Biomembr, 1999. **31**(5): p.
406   419-30.

407   2.   Cannon, B. and J. Nedergaard, *Brown adipose tissue: function and physiological significance.* Physiol Rev,
408   2004. **84**(1): p. 277-359.

409   3.   Kuhnlein, R.P., *Thematic review series: Lipid droplet synthesis and metabolism: from yeast to man. Lipid*
410   *droplet-based storage fat metabolism in Drosophila.* J Lipid Res, 2012. **53**(8): p. 1430-6.

411   4.   McGown, C., A. Birerdinc, and Z.M. Younossi, *Adipose tissue as an endocrine organ.* Clin Liver Dis,
412   2014. **18**(1): p. 41-58.

413   5.   Vaiopoulos, A.G., et al., *The role of adiponectin in human vascular physiology.* Int J Cardiol, 2012. **155**(2):
414   p. 188-93.

415   6.   Nishimura, M., et al., *Adiponectin prevents cerebral ischemic injury through endothelial nitric oxide*
416   *synthase dependent mechanisms.* Circulation, 2008. **117**(2): p. 216-23.

417   7.   Sanchez, J.C., et al., *The mouse SWISS-2D PAGE database: a tool for proteomics study of diabetes and*
418   *obesity.* Proteomics, 2001. **1**(1): p. 136-63.

419   8.   Lanne, B., et al., *Thiourea enhances mapping of the proteome from murine white adipose tissue.*
420   Proteomics, 2001. **1**(7): p. 819-28.

421   9.   Hsieh, C.H., et al., *Altered white adipose tissue protein profile in C57BL/6J mice displaying delipidative,*
422   *inflammatory, and browning characteristics after bitter melon seed oil treatment.* PLoS One, 2013. **8**(9): p.
423   e72917.

424   10. Adachi, J., et al., *In-depth analysis of the adipocyte proteome by mass spectrometry and bioinformatics.*
425   Mol Cell Proteomics, 2007. **6**(7): p. 1257-73.

426   11. Forner, F., et al., *Proteome differences between brown and white fat mitochondria reveal specialized*
427   *metabolic functions.* Cell Metab, 2009. **10**(4): p. 324-35.

428   12. Xie, X., et al., *Characterization of the Human Adipocyte Proteome and Reproducibility of Protein*
429   *Abundance by One-Dimensional Gel Electrophoresis and HPLC-ESI-MS/MS.* J Proteome Res, 2010. **9**(9):
430   p. 4521-34.

431   13. Feist, P.E., et al., *Quantitative proteomic analysis of murine white adipose tissue for peritoneal cancer*
432   *metastasis.* Anal Bioanal Chem, 2018. **410**(5): p. 1583-1594.

433   14. Peinado, J.R., et al., *Proteomic profiling of adipose tissue from Zmpste24-/- mice, a model of lipodystrophy*
434   *and premature aging, reveals major changes in mitochondrial function and vimentin processing.* Mol Cell
435   Proteomics, 2011. **10**(11): p. M111.008094.

436   15. Andrade, J.M., et al., *Proteomic white adipose tissue analysis of obese mice fed with a high-fat diet and*
437   *treated with oral angiotensin-(1-7).* Peptides, 2014. **60**: p. 56-62.

438   16. Kim, S.W., et al., *Differential protein expression in white adipose tissue from obesity-prone and obesity-*
439   *resistant mice in response to high fat diet and anti-obesity herbal medicines.* Cell Physiol Biochem, 2015.
440   **35**(4): p. 1482-98.

441   17. Ke, M., et al., *Differential proteomic analysis of white adipose tissues from T2D KKAy mice by LC-ESI-*
442   *QTOF.* Proteomics, 2017. **17**(5).

443   18. Kim, M.S., et al., *A draft map of the human proteome.* Nature, 2014. **509**(7502): p. 575-81.

444 19. Wilhelm, M., et al., *Mass-spectrometry-based draft of the human proteome.* Nature, 2014. **509**(7502): p.
445   582-7.

446 20. Consortium, E.P., *An integrated encyclopedia of DNA elements in the human genome.* Nature, 2012.
447   **489**(7414): p. 57-74.

448 21. Gilar, M., et al., *Orthogonality of separation in two-dimensional liquid chromatography.* Anal Chem, 2005.
449   **77**(19): p. 6426-34.

450 22. Wang, Y., et al., *Reversed-phase chromatography with multiple fraction concatenation strategy for*
451   *proteome profiling of human MCF10A cells.* Proteomics, 2011. **11**(10): p. 2019-26.

452 23. Song, C., et al., *Reversed-phase-reversed-phase liquid chromatography approach with high orthogonality*
453   *for multidimensional separation of phosphopeptides.* Anal Chem, 2010. **82**(1): p. 53-6.

454 24. Wisniewski, J.R., et al., *Universal sample preparation method for proteome analysis.* Nat Methods, 2009.
455   **6**(5): p. 359-62.

456 25. Schwanhausser, B., et al., *Global quantification of mammalian gene expression control.* Nature, 2011.
457   **473**(7347): p. 337-42.

458 26. Lyons, G.E., et al., *Carbonic anhydrase III, an early mesodermal marker, is expressed in embryonic mouse*
459   *skeletal muscle and notochord.* Development, 1991. **111**(1): p. 233-44.

460 27. Joo, J.I., et al., *Proteomic analysis for antiobesity potential of capsaicin on white adipose tissue in rats fed*
461   *with a high fat diet.* J Proteome Res, 2010. **9**(6): p. 2977-87.

462 28. Aboulaich, N., et al., *Polymerase I and transcript release factor regulates lipolysis via a phosphorylation-*
463   *dependent mechanism.* Diabetes, 2011. **60**(3): p. 757-65.

464 29. Ahmed, M., et al., *Proteomic analysis of human adipose tissue after rosiglitazone treatment shows*
465   *coordinated changes to promote glucose uptake.* Obesity (Silver Spring), 2010. **18**(1): p. 27-34.

466 30. Wang, P., et al., *Profiling of the secreted proteins during 3T3-L1 adipocyte differentiation leads to the*
467   *identification of novel adipokines.* Cell Mol Life Sci, 2004. **61**(18): p. 2405-17.

468 31. Todorcevic, M., et al., *Gene expression profiles in Atlantic salmon adipose-derived stromo-vascular*
469   *fraction during differentiation into adipocytes.* BMC Genomics, 2010. **11**: p. 39.

470 32. Ali Khan, A., et al., *Comparative secretome analyses of primary murine white and brown adipocytes reveal*
471   *novel adipokines.* Molecular & Cellular Proteomics, 2018.

472 33. Trayhurn, P. and J.H. Beattie, *Physiological role of adipose tissue: white adipose tissue as an endocrine*
473   *and secretory organ.* Proc Nutr Soc, 2001. **60**(3): p. 329-39.

474 34. Trayhurn, P. and I.S. Wood, *Adipokines: inflammation and the pleiotropic role of white adipose tissue.* Br J
475   Nutr, 2004. **92**(3): p. 347-55.

476 35. Yue, L., et al., *Divergent effects of peroxisome proliferator-activated receptor gamma agonists and tumor*
477   *necrosis factor alpha on adipocyte ApoE expression.* J Biol Chem, 2004. **279**(46): p. 47626-32.

478 36. Geiger, T., et al., *Comparative proteomic analysis of eleven common cell lines reveals ubiquitous but*
479   *varying expression of most proteins.* Mol Cell Proteomics, 2012. **11**(3): p. M111 014050.

480 37. Kimball, S.R., *Eukaryotic initiation factor eIF2.* Int J Biochem Cell Biol, 1999. **31**(1): p. 25-9.

481 38. Swetha, M. and K.V.A. Ramaiah, *Insulin treatment promotes tyrosine phosphorylation of PKR and inhibits*
482   *polyIC induced PKR threonine phosphorylation.* Arch Biochem Biophys, 2015. **585**: p. 98-108.

483 39. Langin, D., *Adipose tissue lipolysis as a metabolic pathway to define pharmacological strategies against*
484   *obesity and the metabolic syndrome.* Pharmacol Res, 2006. **53**(6): p. 482-91.

485   40.   Williams, A.S., L. Kang, and D.H. Wasserman, *The extracellular matrix and insulin resistance.* Trends
486   Endocrinol Metab, 2015. **26**(7): p. 357-66.
487   41.   Chen, X. and S. Hess, *Adipose proteome analysis: focus on mediators of insulin resistance.* Expert Rev
488   Proteomics, 2008. **5**(6): p. 827-39.
489   42.   Wang, F. and Q. Tong, *SIRT2 suppresses adipocyte differentiation by deacetylating FOXO1 and enhancing
490   FOXO1's repressive interaction with PPARgamma.* Mol Biol Cell, 2009. **20**(3): p. 801-8.
491   43.   Wang, F., et al., *SIRT2 deacetylates FOXO3a in response to oxidative stress and caloric restriction.* Aging
492   Cell, 2007. **6**(4): p. 505-514.
493   44.   Boudina, S. and T.E. Graham, *Mitochondrial function/dysfunction in white adipose tissue.* Experimental
494   Physiology, 2014. **99**(9): p. 1168-1178.
495   45.   Choo, H.J., et al., *Mitochondria are impaired in the adipocytes of type 2 diabetic mice.* Diabetologia, 2006.
496   **49**(4): p. 784-91.
497   46.   De Pauw, A., et al., *Mitochondrial (dys)function in adipocyte (de)differentiation and systemic metabolic
498   alterations.* Am J Pathol, 2009. **175**(3): p. 927-39.
499   47.   Wilson-Fritch, L., et al., *Mitochondrial Biogenesis and Remodeling during Adipogenesis and in Response
500   to the Insulin Sensitizer Rosiglitazone.* Molecular and Cellular Biology, 2003. **23**(3): p. 1085-1094.
501   48.   Cao, Y., H. Wang, and W. Zeng, *Whole-tissue 3D imaging reveals intra-adipose sympathetic plasticity
502   regulated by NGF-TrkA signal in cold-induced beiging.* Protein Cell, 2018. **9**(6): p. 527-539.
503   49.   Qiu, Y., et al., *Eosinophils and type 2 cytokine signaling in macrophages orchestrate development of
504   functional beige fat.* Cell, 2014. **157**(6): p. 1292-308.
505   50.   Giordano, A., A. Frontini, and S. Cinti, *Convertible visceral fat as a therapeutic target to curb obesity.* Nat
506   Rev Drug Discov, 2016. **15**(6): p. 405-24.
507   51.   Harms, M. and P. Seale, *Brown and beige fat: development, function and therapeutic potential.* Nat Med,
508   2013. **19**(10): p. 1252-63.
509   52.   Soni, K.G., et al., *Carboxylesterase 3 (EC 3.1.1.1) is a major adipocyte lipase.* J Biol Chem, 2004. **279**(39):
510   p. 40683-9.
511   53.   Sackmann-Sala, L., et al., *Age-related and depot-specific changes in white adipose tissue of growth
512   hormone receptor-null mice.* J Gerontol A Biol Sci Med Sci, 2014. **69**(1): p. 34-43.
513   54.   Pereira, L., et al., *Pathogenetic sequence for aneurysm revealed in mice underexpressing fibrillin-1.* Proc
514   Natl Acad Sci U S A, 1999. **96**(7): p. 3819-23.
515   55.   Lopez, I.P., et al., *Gene expression changes in rat white adipose tissue after a high-fat diet determined by
516   differential display.* Biochem Biophys Res Commun, 2004. **318**(1): p. 234-9.
517   56.   Takahara, H. and H. Sinohara, *Mouse plasma trypsin inhibitors: inhibitory spectrum of contrapsin and
518   alpha-1-antitrypsin.* Thromb Res, 1982. **27**(1): p. 45-50.
519   57.   Takahara, H. and H. Sinohara, *Inhibitory spectrum of mouse contrapsin and alpha-1-antitrypsin against
520   mouse serine proteases.* J Biochem, 1983. **93**(5): p. 1411-9.
521
522

523 **Figure legends**

524 **Fig. 1 Proteome profile analysis of the normal WAT proteome.**

525 **(A)** Venn diagram of protein identification in three technical replicates. **(B)** Technical variation of

526 the three replicates. **(C)** Quantitative protein abundance range in WAT samples with the iBAQ

527 algorithm.

528 **Fig.2 Venn diagram analysis of mouse WAT proteome.** (A) Venn diagram analysis of present

529 mouse WAT proteome studies. (B) Protein distribution based on abundance of WAT proteome in

530 this study.

531 **Fig.3 Functional analysis of WAT proteome according to protein abundance. (A)** cellular

532 components. **(B)** molecular function. **(C)** biological processes. (D) Canonical pathway of WAT

533 proteome.

534 **Supporting Information**

535 **Table S1** The qualitative results from the WAT proteome from three technical replicates.

536 **Table S2** The list of peptides in the WAT proteome.

537 **Table S3** The list of proteins in the WAT proteome.

538 **Table S4** iBAQ intensity of quantified WAT proteins.

539 **Table S5** IPA annotation of the WAT proteome.

540 **Table S6** The list of proteins with signal peptides.

541 **Supplemental Fig. S1 The mouse gonadal white adipose tissue proteome profile workflow.**

542 **Supplemental Fig. S2 Correlation plot of protein abundance between two runs**

543 **Supplemental Fig. S3 Venn diagram analysis of mouse WAT proteome with high-**

544 **abundance proteins in this study.**

545 **Supplemental Fig.S4 Top canonical pathways in WAT.**

546 **Supplemental Fig.S5 Mitochondrial dysfunction (A) and oxidative phosphorylation (B)**

547 **signaling pathway**. The red-filled graph represents high-abundance protein; the gray one is

548 middle-abundance protein; and the green one is low-abundance protein).

The top ten most abundant proteins in the mouse WAT proteome.

1 **Table 1. The top ten abundant proteins in the mouse WAT proteome.**

Accession number	Name	iBAQ value	Percentage
P07724	Serum albumin	2.87E+05	9.33%
P16015	Carbonic anhydrase 3	1.21E+05	1.68%
O54724	Polymerase I and transcript release factor	8.01E+04	1.67%
P58774	Tropomyosin beta chain	8.72E+04	1.36%
P20152	Vimentin	4.93E+04	1.25%
P31001	Desmin	4.23E+04	1.07%
Q60605	Myosin light polypeptide 6	1.30E+05	1.04%
P37804	Transgelin	8.74E+04	0.93%
P16045	Galectin-1	1.20E+05	0.85%
Q08091	Calponin-1	5.05E+04	0.80%

Proteomic studies on the mouse WAT proteome.

1 **Table 2. Proteomic studies on the mouse WAT proteome.**

NO.	Year	Protein identification	Fraction methods	MS	FDR	Reference
1	2001	61	2D-PAGE	MALDI-TOF-MS		Sanchez et al.[7]
2	2001	108	2D-SDS-PAGE	MALDI-TOF-MS, Q-TOF		Lanne et al.[8]
3	2007	3287	SDS-PAGE followed by LC	LTQ-FTICR		Adachi et al.[10]
4	2009	2434	SDS-PAGE followed by HPLC	LTQ-Orbitrap	Protein level FDR<1%	Forner et al.[11]
5	2010	1493	SDS-PAGE followed by HPLC	LTQ-FTICR	Protein probability score≥99%	Xie et al.[12]
6	2018	2308	low-fraction SDSPAGE gel followed by LC	Q-Exactive	Protein level FDR=1%	Peter et al.[13]
7	2018	6036	RPLC	Triple TOF	Protein level FDR=1%	This study

Figure 1

The mouse white adipose tissue proteome profile workflow.
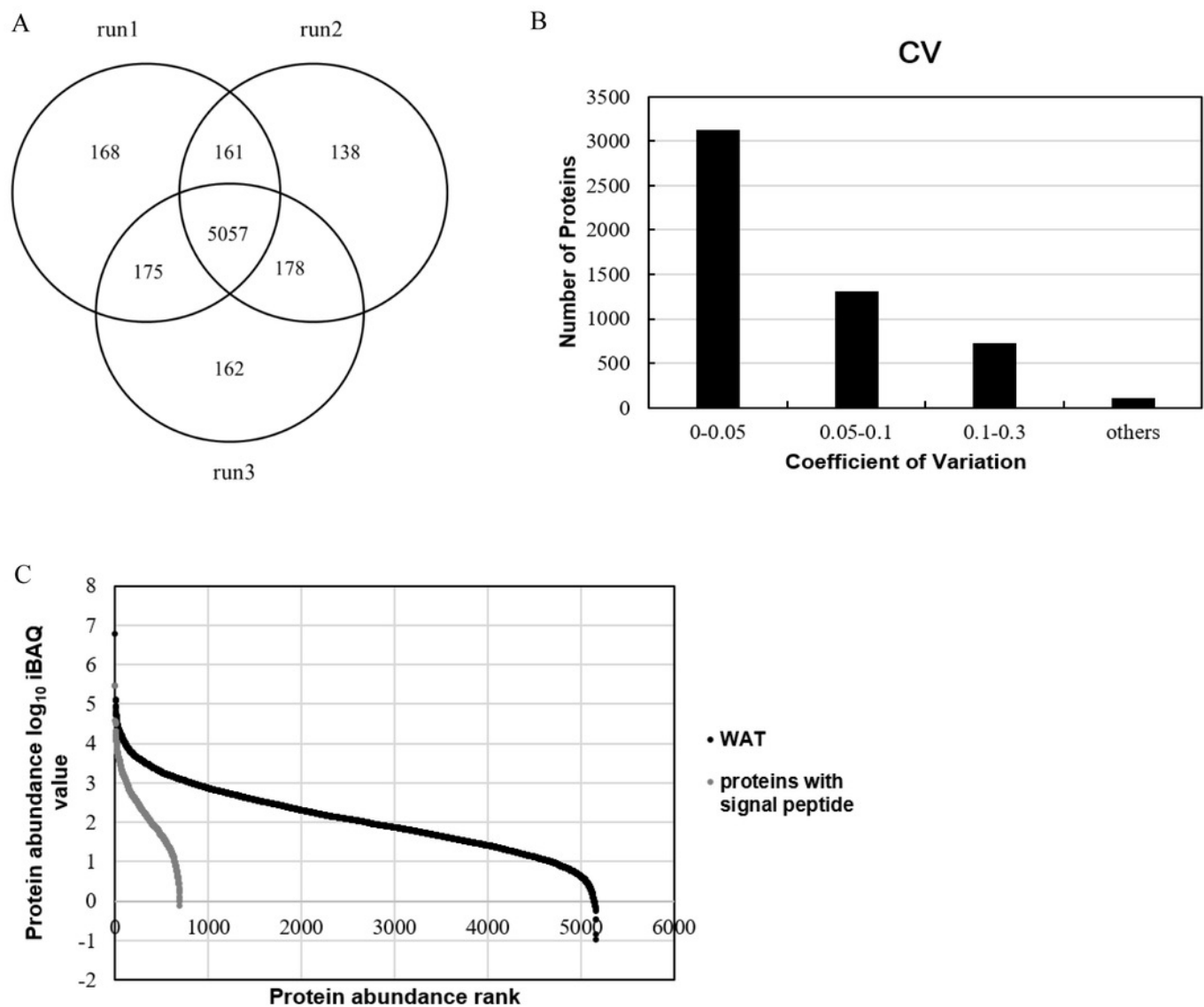
Figure 2

Proteome profile analysis of the normal WAT proteome.

(A) Venn diagram of protein identification in three technical replicates. (B) Technical variation of the three replicates. (C) Quantitative protein abundance range in WAT samples with the iBAQ algorithm. (D) Venn diagram comparing previous proteomic studies with this study.
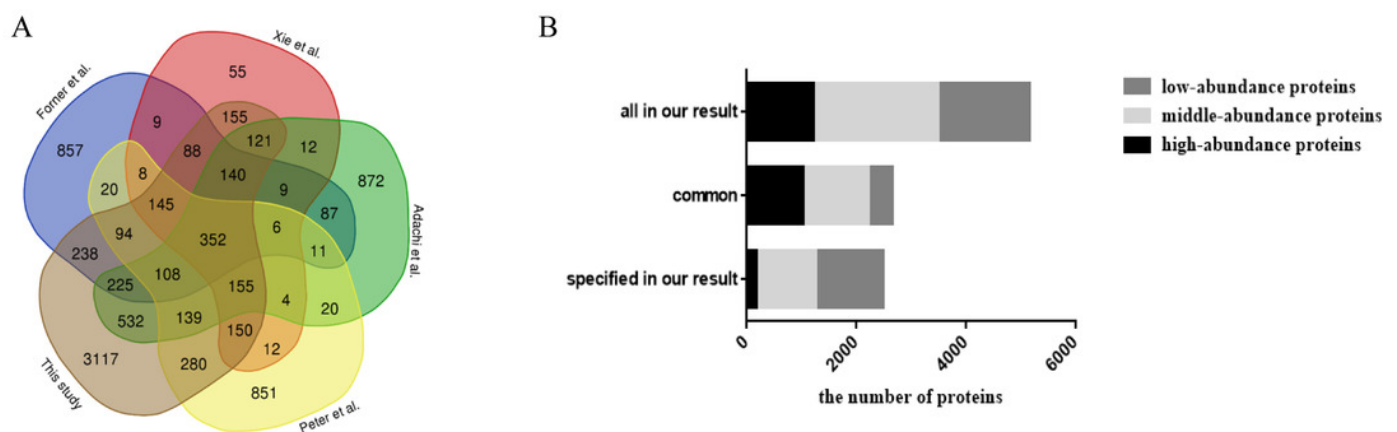
Figure 3

Functional annotation (GO and IPA analysis) of WAT proteome.

(A) cellular components, (B) molecular function, (C)biological processes, (D) top canonical pathway.